MOLECULAR AND CELLULAR BIOLOGY, Apr. 2007, p. 2812–2820 Vol. 27, No. 8
0270-7306/07/$08.00+0 doi:10.1128/MCB.02043-06

Cooperative Roles of Vertebrate Fbh1 and Blm DNA Helicases in Avoidance of Crossovers during Recombination Initiated by Replication Fork Collapse▽†

Masaoki Kohzaki,[1,2] Atsushi Hatanaka,[1] Eiichiro Sonoda,[1] Mitsuyoshi Yamazoe,[1] Koji Kikuchi,[1] Nguyen Vu Trung,[1,3] Dávid Szüts,[4] Julian E. Sale,[4] Hideo Shinagawa,[5] Masami Watanabe,[2] and Shunichi Takeda[1]*

Department of Radiation Genetics, Kyoto University Graduate School of Medicine, Yoshidakonoe, Sakyo-ku, Kyoto 606-8501, Japan[1]; Research Reactor Institute, Kyoto University, Kumatori, Sennan-gun, Osaka 590-0494, Japan[2]; Department of Medical Microbiology, Hanoi Medical University, 01 Ton That Tung, Dong Da, Hanoi, Vietnam[3]; Medical Research Council Laboratory of Molecular Biology, Division of Protein and Nucleic Acid Chemistry, Hills Road, Cambridge CB2 2QH, United Kingdom[4]; and Department of Molecular Microbiology, Research Institute for Microbial Diseases, Osaka University, 3-1 Yamada-oka, Suita, Osaka 565-0871, Japan[5]

Received 1 November 2006/Returned for modification 18 December 2006/Accepted 2 January 2007

Fbh1 (F-box DNA helicase 1) orthologues are conserved from *Schizosaccharomyces pombe* to chickens and humans. Here, we report the disruption of the *FBH1* gene in DT40 cells. Although the yeast *fbh1* mutant shows an increase in sensitivity to DNA damaging agents, *FBH1*$^{-/-}$ DT40 clones show no prominent sensitivity, suggesting that the loss of *FBH1* might be compensated by other genes. However, *FBH1*$^{-/-}$ cells exhibit increases in both sister chromatid exchange and the formation of radial structures between homologous chromosomes without showing a defect in homologous recombination. This phenotype is reminiscent of *BLM*$^{-/-}$ cells and suggests that Fbh1 may be involved in preventing extensive strand exchange during homologous recombination. In addition, disruption of *RAD54*, a major homologous recombination factor in *FBH1*$^{-/-}$ cells, results in a marked increase in chromosome-type breaks (breaks on both sister chromatids at the same place) following replication fork arrest. Further, *FBH1BLM* cells showed additive increases in both sister chromatid exchange and the formation of radial chromosomes. These data suggest that Fbh1 acts in parallel with Bloom helicase to control recombination-mediated double-strand-break repair at replication blocks and to reduce the frequency of crossover.

DNA damage is continuously generated by cellular metabolic products as well as by environmental factors (23) and poses a serious threat to the cells. In cycling cells, it may inhibit the progression of replication forks, resulting in gaps and occasionally double-strand breaks (DSBs) in the daughter strands (4, 34). To release replication blocks and thereby prevent DSBs, cells have evolved two major repair pathways, translesion DNA synthesis and homologous recombination (HR) (15). Translesion synthesis is carried out by a number of specialized translesion synthesis DNA polymerases, which are able to synthesize directly across damaged DNA bases. As an alternative to translesion synthesis, bypass can be effected by a form of HR involving a transient template switch from damaged strand to the newly synthesized daughter strand on the sister chromatid (16). HR is also required for repair of DSBs arising at collapsed replication forks, caused by DNA-damaging agents such as the DNA topoisomerase I inhibitor camptothecin (1, 14). This chemotherapeutic agent covalently attaches to topoisomerase I, allowing it to cleave but not religate DNA. Upon encounter with a replication fork, the topoisomerase I-cleaved DNA complex induces a single-end break (4, 8, 37). Restart of replication from these single-end breaks requires HR with the intact sister chromatid.

The initial step of recombination-mediated DSB repair involves processing of the DSBs to produce a 3′ single-strand overhang, followed by polymerization of Rad51 on the single-stranded DNA. In concert with Rad54 (2, 31, 38), the resulting nucleoprotein filament facilitates the homology search and pairing with the intact duplex DNA donor to form a D-loop structure. Following DNA synthesis from the invading 3′ end, the strand is dissociated from the D loop and rehybridizes with the 3′ single-strand tail of the other side of the DSB. This type of HR-dependent DSB repair is called synthesis-dependent strand annealing, which is thought to account for a majority of mitotic HR (18, 30). In contrast to synthesis-dependent strand annealing, which does not result in the formation of crossovers, strand exchange following D-loop formation results in the formation of a Holliday junction. Holliday junctions can be resolved by incisions at the junction, which can result in crossover formation (24). It has also been proposed that double Holliday junctions are dissolved by the concerted action of the RecQ helicase Blm and topoisomerase III α (42).

The *BLM* helicase is mutated in Bloom's syndrome. This rare autosomal recessive genetic disease features an elevated rate of sister chromatid exchange (SCE), frequent recombination between allelic genes, increased genome instability, and a

* Corresponding author. Mailing address: Department of Radiation Genetics, Faculty of Medicine, Kyoto University, Sakyo-ku, Kyoto 606-8501, Japan. Phone: 81 75 753 4410. Fax: 81 75 753 4419. E-mail: stakeda@rg.med.kyoto-u.ac.jp.

† Supplemental material for this article may be found at http://mcb.asm.org/.

▽ Published ahead of print on 5 February 2007.

high incidence of tumorigenesis (9). The Bloom helicase is one of five human RecQ helicases, which share 3′-to-5′ DNA helicase activity as well as structural homology. Yeast species, on the other hand, have only a single orthologous gene, Sgs1 in *Saccharomyces cerevisiae* and Rqh1 in *Schizosaccharomyces pombe* (12). Although these RecQ family helicases have been implicated in the initiation of replication restart without crossover and resolution of recombination intermediates (32, 40, 42), their function remains poorly understood even in yeast due to the complexity of repair reactions following replication block and the lack of an appropriate phenotypic assay to monitor the late steps of HR in vivo. Likewise, the detailed molecular function of the mammalian RecQ helicase remains elusive.

The *FBH1* (F-box DNA helicase 1) gene was recently identified in *Schizosaccharomyces pombe*, and its orthologous genes are conserved in chickens, mice, and humans but not in budding yeast (22). Fbh1 belongs to the superfamily 1 helicase and has unwinding activity with a 3′-to-5′ direction. Fbh1 is structurally similar to the Srs2 DNA helicase family, which includes the PcrA, Rep, and UvrD helicases (43). Fbh1 also contains an F box toward its N terminus, suggesting that Fbh1 acts as a ubiquitin ligase (E3) in the SCF complex, although the substrate of the ubiquitin ligase has not been determined (21). The *S. pombe fbh1* mutant is moderately sensitive to UV; methylmethane sulfonate (MMS), an alkylating agent; and γ-rays. Genetic studies show that Fbh1 is essential for viability in the absence of Rqh1 and that this lethality is suppressed by additional inactivation of Rad51 paralogs, which promote an early step of HR. Thus, Fbh1 may affect recombination-dependent repair downstream of Rhp51 (*S. pombe* Rad51 ortholog), probably by promoting the processing of recombination intermediates. This notion is supported by the finding that spontaneous Rad51 focus formation was enhanced in an *fbh1*-deficient *S. pombe* mutant (27, 29). Therefore, Fbh1 may share a redundant function with Srs2 in *S. pombe*.

In this study, we established *FBH1*-deficient DT40 cells to investigate Fbh1 function in vertebrate cells. The resulting *FBH1*$^{-/-}$ cells exhibited essentially a normal phenotype. The functional overlap between yeast Fbh1 and Rqh1 led us to investigate whether other genes compensate for the loss of Fbh1 in DT40 cells. To this end, we disrupted the *FBH1* gene in DT40 lines mutant for the *FANCC*$^{-}$, *RAD18*$^{-/-}$, *RAD54*$^{-/-}$, and *BLM*$^{-/-}$ genes (5, 13, 17, 44). We show that although inactivation of *FBH1* did not reduce the efficiency of HR, Fbh1 acts in parallel with Blm and restricts the extent of strand exchange during recombination initiated by stalled replication, thereby reducing the frequency of crossover formation.

MATERIALS AND METHODS

Cloning of the chicken *FBH1* gene. A chicken *FBH1* cDNA was partially amplified from chicken testis cDNA by reverse transcriptase PCR (RT-PCR) with the primer pair 5′-AAATCATGGCTTTTGCNGGNACTGG-3′ and 5′-CACCTCGGAAGGAATAGATCTGCTG-3′, the design of which was based on conserved sequences between the human and xenopus *FBH1* homologs. Rapid amplification of cDNA ends was carried out to isolate the 3′ and 5′ termini of the chicken *FBH1* transcript. Full-length cDNA of chicken *FBH1* (Gd*FBH1*) was amplified from chicken testis cDNA by RT-PCR with a primer pair, 5′-AGAAAATGCACCTTACAGCTG-3′ and 5′-GCAATGGCTCTGGGAGTTGG-3′. An amplified 3-kb fragment was subcloned into a pCR2.1-TOPO vector (Invitrogen) and sequenced.

Construction of targeting vectors. The positions of exons and introns were determined by base sequencing. Genomic DNA sequences were amplified with two sets of primers, 5′-CTGCCACAGATATGCTAGAG-3′ and 5′-TTTCCCATGTACTCATCCTC-3′ plus 5′-GACTTTGTGGATGTACCGTG-3′ and 5′-ATGGAGCCAAAACGCTTCTG-3′, for the left and right arms, respectively, of the disruption construct. Amplified PCR products (1.5 kb for the left arm and 3.5 kb for the right arm) were cloned into pCR2.1-TOPO vector (Invitrogen). The 3.5-kb KpnI (blunt ended)-NotI fragment was cloned into the EcoRV-NotI site of pCR2.1 containing the 1.5-kb left arm sequence. The BamHI site was used to insert marker gene cassettes, *hisD* and *bsr* selection marker genes flanked by *loxP* sequences, to generate the *FBH1-hisD* and *FBH1-bsr* gene disruption constructs, respectively (3). The *puro* marker gene was inserted into the BamHI site to generate the *FBH1-puro* gene disruption construct. The 0.5-kb fragment generated by PCR amplification of genomic DNA using the primers 5′-TTCAGGAAGAGCCCATCGTG-3′ and 5′-AATGTCCCCACTGAAACAGG-3′ was used as a probe for Southern blot analysis to screen gene-targeting events. Plasmids were linearized prior to transfection into DT40 cells; *FBH1-hisD* and *FBH1-bsr* were digested with XhoI, and *FBH1-puro* was digested with KpnI.

Generation of gene-disrupted cells. Wild-type DT40 cells that stably express the CreER chimeric recombination enzyme were transfected sequentially with *FBH1-bsr* and *FBH1-hisD* targeting constructs to obtain *FBH1*$^{+/-}$ and *FBH1*$^{-/-}$ cells (Fig. 1A) (10, 25). Stable expression of CreER did not affect the viability of the cells or their sensitivity to DNA damaging agents (data not shown). Targeting events were verified by the appearance of a 6-kb band and the disappearance of a 9-kb band in Southern blot analysis of EcoRI-digested genomic DNA (Fig. 1B). Gene disruption of each transfected clone was confirmed by RT-PCR analysis of *FBH1* gene transcription. The primers used for RT-PCR were the forward primer 5′-TTGAGCGTGGTCAGATAGTG-3′ and the reverse primer 5′-CACCTCGGAAGGAATAGATCTGCTG-3′ (Fig. 1D). β-Actin transcripts were analyzed as positive controls for RT-PCR analysis. Identified *FBH1*$^{-/-}$ clones were treated with 100 nM tamoxifen to exclude *bsr* and *hisD* marker cassettes from chromosomal DNA (44). The resulting *FBH1*$^{-/-}$ cells were sequentially transfected with *BLM-hisD* and *BLM-bsr* targeting constructs to obtain *FBH1*$^{-/-}$ *BLM*$^{+/-}$ and *FBH1*$^{-/-}$ *BLM*$^{-/-}$ clones, respectively (41). Likewise, *RAD54-hisD* and *RAD54-puro* targeting constructs were used for generating *FBH1*$^{-/-}$ *RAD54*$^{-/-}$ cells (5). The *FANCC* gene, which is encoded in a single sex chromosome, was disrupted in *FBH1*$^{-/-}$ cells by using the *FANCC-puro* plasmid (13). *RAD18*$^{-/-}$ cells were sequentially transfected with *FBH1-bsr* and *FBH1-puro* targeting constructs to obtain *FBH1*$^{-/-}$ *RAD18*$^{+/-}$ and *FBH1*$^{-/-}$ *RAD18*$^{-/-}$ clones, respectively (44). To express chicken Fbh1, its cDNA was inserted into the p176 expression vector containing the Neo selection marker gene (10). The expression plasmid was linearized with PvuI prior to transfection into cells. The conditions for cell culture, selection, and DNA transfections have been described previously (35).

Proliferation analysis and colony formation assay. A colony formation assay was performed as described previously (28). To measure the sensitivity to camptothecin, cells were plated in methylcellulose medium containing camptothecin. The experimental methods for cell counting and cell cycle analysis were described previously (39).

Measurement of SCE levels. Measurement of SCE levels was carried out as described previously (28, 44). To measure camptothecin-induced SCE, cells were labeled with bromodeoxyuridine (BrdU) for two cell cycle periods (~20 h) and treated with 5 nM camptothecin for the last 9 h. To measure SCE induced by UV, cells were treated with 0.25 J/m^2 of UV and incubated with 10 uM BrdU for 20 h. The cells were incubated with Colcemid to enrich metaphase cells for the last 3 h before harvest.

Chromosomal aberration analysis. Preparation of chromosome spreads and karyotype analysis were performed as described previously (35, 44). To measure camptothecin-induced chromosomal aberrations, cells were incubated with 10 nM camptothecin for 9 h before harvest and fixation. To analyze UV-induced chromosomal aberrations, cells were suspended in 1 ml of phosphate-buffered saline, spread onto six-well plates, and exposed to 1 J/m^2 UVC, followed by the addition of 5 ml of the complete medium. Cells were harvested every 3 h for 15 h. To enrich mitotic cells, cells were exposed to Colcemid for the last 3 h.

Measurement of targeted integration frequencies. HR was evaluated by the following three methods. First, the frequency of I-SceI restriction enzyme-induced HR was measured as described previously (11, 19). The assay plasmid was inserted into the *OVALBUMIN* locus. Second, to analyze targeted integration events at the *OVALBUMIN*, *RAD54*, and *CENP-H* loci, each disruption construct was transfected into cells. Gene targeting events were identified by either Southern blot analysis or FACS analysis of EGFP–*CENP-H* fusion protein ex-

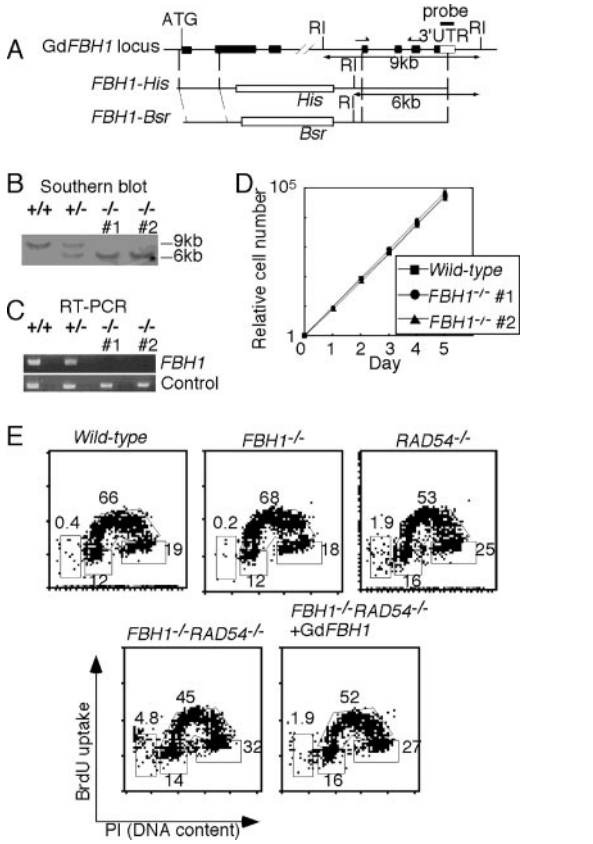

FIG. 1. Gene targeting of the *FBH1* locus. (A) Schematic representation of a part of the *FBH1* locus and the targeting constructs. The *FBH1* replacement constructs, which contain a *bsr* or *hisD* selection marker gene, were used to disrupt the *FBH1* locus. The filled box represents the *FBH1* exons. RI, EcoRI. (B) Southern blot analysis of EcoRI-digested DNA using the probe indicated in panel A. (C) RT-PCR analysis of total RNA using the primers shown in panel A. The coding region of the chicken β-actin gene was amplified as a control. (D) Normal growth kinetics of *FBH1*$^{-/-}$ cells. (E) Cell cycle distribution of the indicated cell lines. Cells were stained with FITC–anti-BrdU antibody (*y* axis, log scale) to detect BrdU uptake and with propidium iodide to measure the total DNA (*x* axis, linear scale). The upper gate identifies cells incorporating BrdU (~S phase), the lower left gate identifies G_1 cells, and the lower right gate displays G_2/M cells. The sub-G_1 fraction reflects dead cells. The numbers given in the boxes indicate the percentages of gated events.

pression (20). Lastly, HR-mediated immunoglobulin V (IgV) diversification (Ig gene conversion) was monitored, as described previously (6). To this end, *FBH1*$^{-/-}$ clones were generated from wild-type DT40 cells that carry a specific frameshift mutation. The rate of Ig gene conversion was assessed by measuring the gain of surface IgM expression during the 3-week period with clonal expansion.

Nucleotide sequence accession number. The chicken *FBH1* cDNA sequences have been submitted to the GenBank database under accession number EF066526.

RESULTS

No apparent defect in HR in the absence of Fbh1. The chicken *FBH1* encodes a polypeptide comprised of 1,012 amino acids that has 55%, 50%, and 26% identity at the amino acid level to the human, mouse, and *S. pombe* orthologs, respectively. Gene-targeting constructs were generated to delete amino acids 118 to 875, including both the F-box domain and five helicase motifs (Ia, Ib, II, III, IV) of the *FBH1* gene (Fig. 1A; also see Fig. S1 in the supplemental material). Two independent *FBH1*$^{-/-}$ clones were identified by Southern blot analysis (Fig. 1B). Gene disruption of these clones was verified by RT-PCR (Fig. 1C). *FBH1*$^{-/-}$ cells were able to proliferate with normal kinetics (Fig. 1D). Flow cytometric analysis of BrdU pulse-labeled cells showed a normal cell cycle distribution (Fig. 1E).

We evaluated the capability of HR in *FBH1*$^{-/-}$ cells by using the following phenotypic assays: sensitivity to DNA damaging agents (Fig. 2), gene-targeting frequency (Table 1), HR-mediated repair of DSBs induced by the I-SceI restriction enzyme, HR-dependent diversification of the Ig gene (Ig gene conversion), and the kinetics of Rad51 subnuclear focus formation. *FBH1*$^{-/-}$ cells were tolerant to γ-rays, MMS, UV, and cisplatin, as were wild-type cells (Fig. 2A to D), while exhibiting modest sensitivity to camptothecin (Fig. 2E). The efficiency of both gene targeting (Table 1) and HR-dependent DSB repair following I-SceI expression (Fig. 3A) was indistinguishable between wild-type and *FBH1*$^{-/-}$ cells. Likewise, *FBH1*$^{-/-}$ cells appear to undergo Ig gene conversion with normal kinetics (data not shown). The kinetics of subnuclear Rad51 focus formation following γ-irradiation were the same between wild-type and *FBH1*$^{-/-}$ cells during the cell cycle and at 3 h, 6 h (Fig. 3B), and 24 h (data not shown) after γ-irradiation. Collectively, *FBH1*$^{-/-}$ cells can perform HR reactions with normal kinetics, which agrees with the previous finding of no effect on spontaneous and DNA damage-induced recombination in Fbh1-deficient yeast (29).

Deletion of the *FBH1* gene has no significant effect on *FANCC*- or *RAD18*-deficient cells. Despite apparently normal HR, *FBH1*$^{-/-}$ cells exhibited significant increases in the level of spontaneously arising SCE (Fig. 3C and D). This increased SCE was reversed by reconstitution of *FBH1*$^{-/-}$ cells with chicken *FBH1* cDNA (data not shown). Taking the normal HR efficiency of *FBH1*$^{-/-}$ cells into account, the increased spontaneous SCE suggests either an increase in the amount of endogenous DNA damage that stimulates SCE or an elevated ratio of crossover-type HR relative to non-crossover-type HR. To gain an insight into the increased spontaneous SCE, we measured SCE induced by camptothecin and UV (Fig. 3C and D), which result in DSBs and single-strand gaps, respectively, when replication forks encounter the damaged sites. Subtraction of spontaneous SCE from camptothecin-induced SCE indicates that camptothecin-induced SCE was at the same level in wild-type and *FBH1*$^{-/-}$ cells (Fig. 3C). In contrast, UV induced a moderately higher level of SCE in *FBH1*$^{-/-}$ cells than in wild-type cells (Fig. 3D). Thus, we suggest that single-strand gaps spontaneously formed at stalled replication forks stimulate crossover-type HR more frequently in the absence of Fbh1. Further, camptothecin-induced DSBs may not be repaired adequately by HR and may lead to cell death in *FBH1*$^{-/-}$ cells (Fig. 2E).

The elevation of spontaneous SCE led us to explore the functional interactions between Fbh1 and either FancC or Rad18, because cells deficient in these proteins exhibit increased levels of spontaneous SCE (13, 44). To this end, we made *FBH1*$^{-/-}$ *FANCC*$^{-}$ and *FBH1*$^{-/-}$ *RAD18*$^{-/-}$ DT40 cells. Inactivation of *FBH1* had no significant impact on

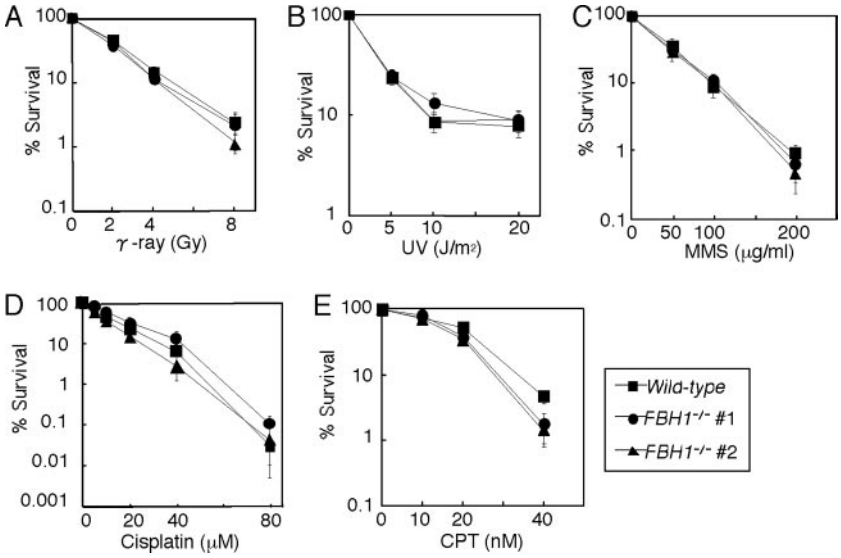

FIG. 2. Sensitivities of the *FBH1* mutant to genotoxic stresses. The indicated genotypes of cells were exposed to γ-rays (A) and UV (B), after a 1-h treatment with MMS (C) and cisplatin (D) and after continuous exposure to camptothecin (CPT) (E). The doses of genotoxic agents are displayed on the *x* axes on a linear scale, while the fractions of surviving colonies are displayed on the *y* axes on a logarithmic scale. Error bars show the standard error of the mean for at least three independent experiments.

FANCC^{-} and *RAD18*$^{-/-}$ cells in terms of cellular sensitivity to cisplatin and MMS (see Fig. S2A and C and Fig. S3A in the supplemental material; also data not shown). On the other hand, *FBH1*$^{-/-}$ *RAD18*$^{-/-}$ cells exhibited slightly higher UV sensitivity than did *RAD18*$^{-/-}$ cells (see Fig. S2D in the supplemental material). In addition, camptothecin sensitivity and spontaneous SCE were increased in *FBH1*$^{-/-}$ *RAD18*$^{-/-}$ and *FBH1*$^{-/-}$ *FANCC*$^{-}$ cells compared with each single mutant (see Fig. S2B and S3B in the supplemental material; also data not shown). These observations indicate no significant functional overlap between Fbh1 and either Rad18 or FancC in suppression of SCE.

Synergistic effect of defective *FBH1* and *RAD54* on genome instability and hypersensitivity to camptothecin. Given that the SCE phenotype of *FBH1*$^{-/-}$ cells suggested that recombination events more frequently resulted in crossover, we sought to test the relationship between Fbh1 and the core recombination factor Rad54 (5). *FBH1*$^{-/-}$ *RAD54*$^{-/-}$ cells grew more slowly, displaying a significant fraction of dying cells compared to each single mutant (Fig. 1E and 4A). Likewise, in *FBH1*$^{-/-}$ *RAD54*$^{-/-}$ cells, higher fractions in the sub-G_1 and G_2 phases were elevated in comparison to the *FBH1*$^{-/-}$ and *RAD54*$^{-/-}$ single mutants (Fig. 1E). As expected, the level of spontaneous SCE was reduced by deletion of the *RAD54* gene in *FBH1*$^{-/-}$ cells (data not shown). Collectively, deletion of *FBH1* in a *RAD54*$^{-/-}$ background compromises genome stability, leading to stimulation of a G_2 damage checkpoint and apoptosis.

TABLE 1. Targeted integration frequencies[a]

Genotype	No. of targeted clones/no. of drug-resistant clones analyzed (%) at the indicated locus			
	OVALBUMIN	*RAD54*	*CENP-H*	
			Expt 1	Expt 2
Wild type	46/47 (97.8)	21/52 (40.4)	19/22 (86.4)	16/29 (55.2)
FBH1$^{-/-}$ (1)	44/46 (95.6)	ND	32/60 (53.3)	14/27 (51.8)
FBH1$^{-/-}$ (2)	35/36 (97.2)	6/36 (16.7)	46/73 (63.0)	28/45 (62.2)

[a] Wild-type and *FBH1*$^{-/-}$ cells were transfected with targeting constructs of the indicated loci. ND, not determined.

FBH1$^{-/-}$ *RAD54*$^{-/-}$ cells were more sensitive to camptothecin than was either single mutant (Fig. 4B). On the other hand, cellular sensitivity to cisplatin (Fig. 4C), γ-rays, and MMS (data not shown) was indistinguishable between *RAD54*$^{-/-}$ and *FBH1*$^{-/-}$ *RAD54*$^{-/-}$ cells. To assess the cause of cellular hypersensitivity to camptothecin, chromosomal aberrations were monitored following exposure of cells to camptothecin (Fig. 4D). In agreement with colony survival data, the *FBH1*$^{-/-}$ *RAD54*$^{-/-}$ cells exhibited a marked increase in camptothecin-induced chromosomal aberrations compared to *RAD54*$^{-/-}$ cells (Fig. 4D). The number of chromosomal aberrations, as well as camptothecin sensitivity, was reversed by ectopic expression of chicken *FBH1* cDNA (Gd*FBH1*) in *FBH1*$^{-/-}$ *RAD54*$^{-/-}$ cells (Fig. 4B and D). It should be noted that camptothecin-induced chromosome-type breaks (DSBs at the same position on two sister chromatids) were significantly increased in *FBH1*$^{-/-}$ *RAD54*$^{-/-}$ cells in comparison with *RAD54*$^{-/-}$ cells. Since camptothecin induces DSBs in one of the two sister chromatids and subsequently stimulates HR with the other intact sister, DSBs at the same position in two sister chromatids, i.e., chromosome-type breaks, indicate that sister recombination is not efficiently completed in *FBH1*$^{-/-}$ *RAD54*$^{-/-}$ cells, leading to DSBs in both sister chromatids during the S and G_2 phases (35).

This raises two hypotheses concerning the function of Fbh1 in DSB repair. First, both Fbh1 and Rad54 may be involved in the same stage of HR, with Fbh1 acting as a backup for Rad54-dependent HR. Alternatively, Fbh1 may prevent the formation of abnormal recombination intermediates, which lead to chromosome-type breaks in the absence of Rad54. To test the former hypothesis, we assayed HR in *RAD54*$^{-/-}$ and *FBH1*$^{-/-}$

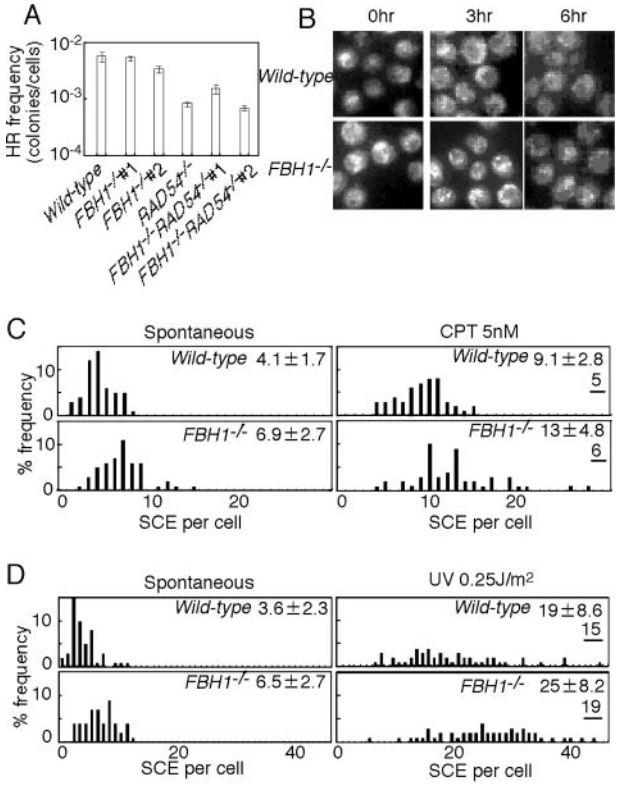

FIG. 3. No significant defect in HR in *FBH1*$^{-/-}$ cells. (A) I-SceI-induced gene conversion assay with the indicated genotypes. The frequency of HR-dependent double-strand-break repair is shown as the number of G418-resistant colonies per 5×10^6 cells (white bars). The experiments were done at least three times. (B) Rad51 focus formation with the indicated genotypes before and at 3 and 6 h after 4 Gy γ-irradiation. (C) Spontaneous and 5 nM camptothecin (CPT)-induced SCE events in the macrochromosomes of 50 metaphase cells. Means ± standard errors are shown in the upper right corner. Underlined numbers indicate subtraction of spontaneous SCE from SCE following CPT treatment. The level of spontaneous SCE in *FBH1*$^{-/-}$ cells significantly differs from that in wild-type cells ($P < 0.0001$). The level of CPT-induced SCE was indistinguishable between wild-type and *FBH1*$^{-/-}$ cells ($P < 0.0001$). Statistical significance was calculated by the Mann-Whitney nonparametric U test (36). (D) UV-induced SCE (0.25 J/m^2) is shown as in panel C. The level of UV-induced SCE was indistinguishable between wild-type and *FBH1*$^{-/-}$ cells ($P < 0.0004$).

RAD54$^{-/-}$ cells by monitoring the repair of I-SceI induced DSBs. Deletion of *FBH1* did not further diminish the capability of HR in *RAD54*$^{-/-}$ cells (Fig. 3A). In addition, Rad51 focus formation following γ-irradiation and camptothecin was comparable in *RAD54*$^{-/-}$ and *FBH1*$^{-/-}$ *RAD54*$^{-/-}$ clones (data not shown). These data are consistent with disruption of *FBH1* resulting in the formation of recombination intermediates that are preferentially resolved with crossover and which lead to chromosome-type breaks in the absence of Rad54.

Complementary role of Fbh1 and Blm in releasing the DNA replication block. The synthetic lethality of the *fbh1* and *rqh1* mutations in yeast, as well as an increase in the level of spontaneous SCE in Fbh1-deficient DT40 clones, prompted us to disrupt the *BLM* gene in *FBH1*$^{-/-}$ cells (9, 17, 41). Unlike in *S. pombe*, *FBH1*$^{-/-}$ *BLM*$^{-/-}$ DT40 cells were able to proliferate with the same kinetics as *BLM*$^{-/-}$ cells (Fig. 5A), but

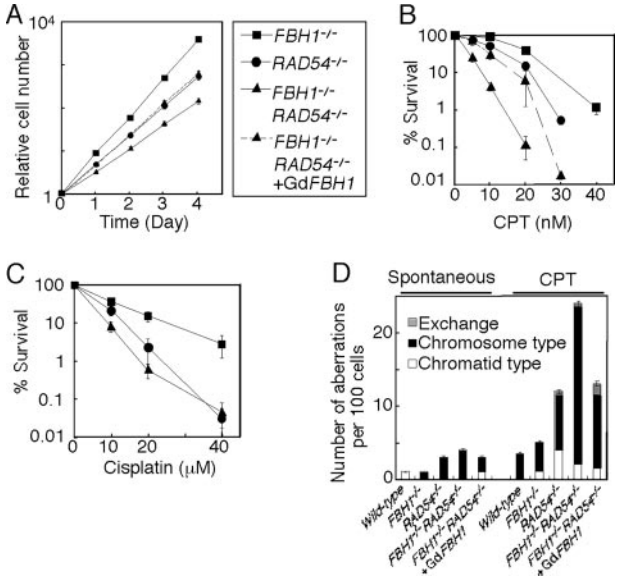

FIG. 4. *FBH1*$^{-/-}$ *RAD54*$^{-/-}$ cells display genome instability and hypersensitivity against camptothecin (CPT). (A) Growth curves of cells of the indicated genotypes. Results were obtained from at least three independent experiments. (B and C) Colony survival assay after treatment with CPT and cisplatin performed as described for Fig. 2. Error bars show the standard error of the mean for at least three independent experiments. (D) Chromosome aberrations before and following 10 nM CPT treatment for 9 h with the indicated genotypes.

FBH1$^{-/-}$ *BLM*$^{-/-}$ cells were considerably more sensitive to camptothecin than was either single mutant (Fig. 5B). Conversely, the sensitivity of *FBH1*$^{-/-}$ *BLM*$^{-/-}$ cells to UV, MMS, and cisplatin was the same as that of *BLM*$^{-/-}$ cells (Fig. 5C and D and data not shown). Thus, Fbh1 may substitute for the

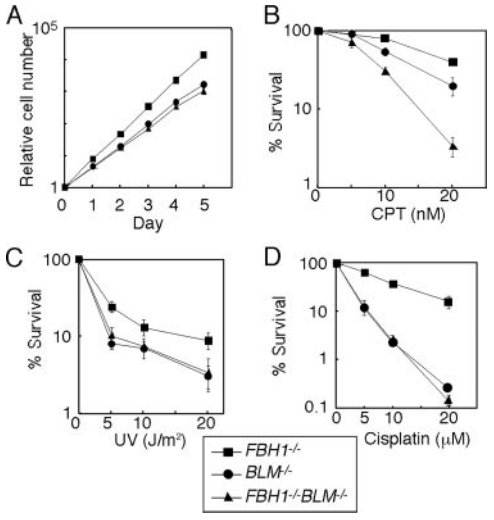

FIG. 5. Combined mutations of the *FBH1* and *BLM* genes synergistically elevate sensitivity to camptothecin (CPT). (A) Growth curves of cells of the indicated genotypes. (B to D) Colony survival assay after treatment with CPT, UV, and cisplatin performed as described for Fig. 2. Error bars show the standard error of the mean for at least three independent experiments.

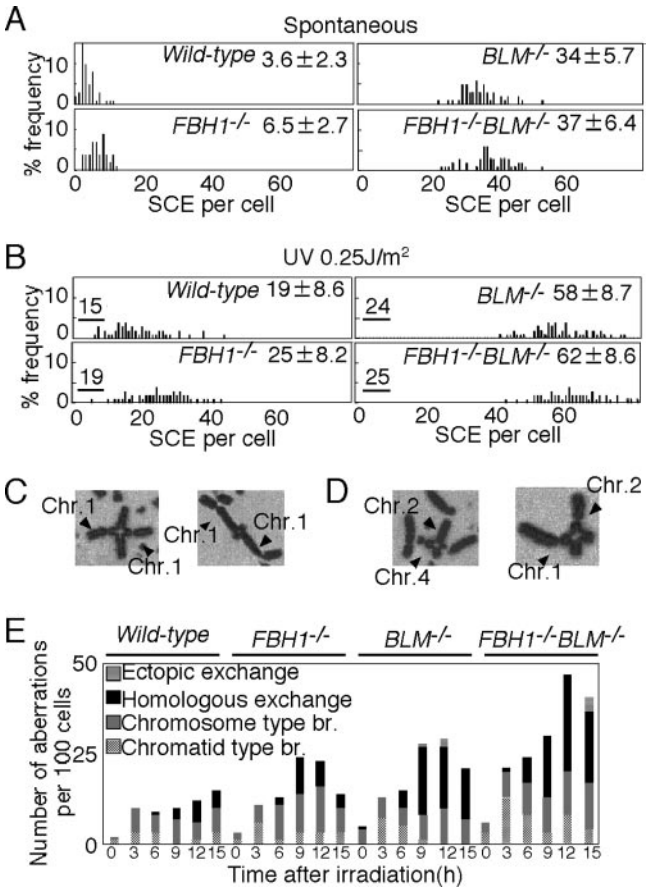

FIG. 6. Increased genome instability of *FBH1*$^{-/-}$ *BLM*$^{-/-}$ cells observed in both UV-induced SCE and exchange between homologous chromosomes. Cells were labeled with BrdU during two cell cycle periods with (B) or without (A) prior UV treatment (0.25 J/m^2). Spontaneous and UV-induced SCEs in the macrochromosomes of 50 metaphase cells were counted. Underlined numbers indicate subtraction of spontaneous SCE from SCE following UV. Histograms show the distribution of cells with the indicated numbers of SCEs per cell. The mean number of SCEs per cell ± standard error is shown in each histogram. The level of spontaneous SCE in *BLM*$^{-/-}$ cells significantly differs from that in *FBH1*$^{-/-}$ *BLM*$^{-/-}$ cells ($P < 0.02$). The level of UV-induced SCE was distinguishable between *BLM*$^{-/-}$ and *FBH1*$^{-/-}$ *BLM*$^{-/-}$ cells ($P < 0.03$), though it may have reached a plateau level. Statistical significance was calculated by the Mann-Whitney nonparametric U test. (C) Representative homologous chromosome exchange in *FBH1*$^{-/-}$ *BLM*$^{-/-}$ cells. Arrowheads indicate chromosome 1. (D) Example of nonhomologous exchange events between chromosomes 1 and 2 and between chromosomes 2 and 4 shown by arrowheads. (E) Frequency of chromosomal aberrations in mitotic cells harvested at indicated times after exposure of asynchronous cell populations to 1 J/m^2 UV. Chromosome aberrations were scored for 100 metaphase cells. All samples were treated with Colcemid for the last 3 h prior to harvest of cells.

loss of Blm, particularly when DSBs occur as a consequence of a replication block.

To further explore the functional overlap between Fbh1 and Blm, we examined SCE and mitotic exchanges between homologous chromosomes, because a significant increase in these two types of crossovers is the characteristic feature of *BLM*-deficient cells (17, 41). *FBH1*$^{-/-}$ and *BLM*$^{-/-}$ DT40 cells showed 1.8- and 9.4-fold-higher numbers of spontaneous SCE events than did wild-type cells, respectively (Fig. 6A). The *FBH1*$^{-/-}$ *BLM*$^{-/-}$ cells displayed further increases in the level of spontaneous SCE. We next examined the level of UV-induced SCE (Fig. 6B). The induction of SCE tended to be higher in *FBH1*$^{-/-}$ and *FBH1*$^{-/-}$ *BLM*$^{-/-}$ cells than in wild-type and *BLM*$^{-/-}$ cells, respectively (Fig. 6B); the number of SCEs in a UV-irradiated *BLM*$^{-/-}$ cell is likely to be saturated, making definitive quantitative measurements unreliable.

We monitored mitotic chromosome aberrations with time following UV irradiation (Fig. 6C to E). Mitotic cells were collected every 3 h from 0 to 15 h after 1 J/m^2 UVC irradiation of asynchronous cells. Cells entering metaphase at 0 to 6 h and 9 to 12 h after UV irradiation reflect cells that received UV irradiation in the late S to G_2 phase and the G_1 to early S phase, respectively (17). UV irradiation increased exchange between homologous chromosomes, i.e., symmetrical chromosomal quadriradials (Fig. 6C), but did not increase exchange between different chromosomes (Fig. 6D) 9 to 12 h after UV irradiation in asynchronous wild-type cells (i.e., cells that were exposed to UV in G_1 to early S phase). These chromosomal quadriradials may result from persisting Holliday junctions formed at sites of replication stalled by UV-induced DNA damage. As expected, *BLM*$^{-/-}$ cells exhibited a marked increase in the number of homologous chromosome exchanges in comparison to wild-type cells (Fig. 6E). This type of chromosomal aberration depends on HR, because deletion of HR factors such as *RAD54* and *XRCC3* in *BLM*$^{-/-}$ cells reduced the formation of symmetrical chromosomal quadriradials by ~10-fold (M. Seki, personal communication). Like *BLM*$^{-/-}$ cells, *FBH1*$^{-/-}$ cells displayed an increase in homologous chromosome exchange. Furthermore, concurrent deletion of *FBH1* and *BLM* had an additive effect on UV-induced quadriradial formation compared to *FBH1*$^{-/-}$ and *BLM*$^{-/-}$ single mutant cells. The total numbers of chromosomal quadriradials were 15 (wild type), 23 (*FBH1*$^{-/-}$), 56 (*BLM*$^{-/-}$), and 72 (*FBH1*$^{-/-}$ *BLM*$^{-/-}$) per 600 metaphase cells in each genotype. These results suggest a possible involvement of the Fbh1 helicase, in parallel with the Blm helicase, in resolving otherwise toxic recombination intermediates produced at the sites of stalled replication forks.

DISCUSSION

Role for vertebrate Fbh1 during DNA replication. As shown in Fig. 7, there are some processes to restrict the extent of strand exchange during recombination produced at the sites of stalled replication forks, resulting in a reduced frequency of crossover formation. Although several DNA helicases have been involved in these processes, the precise mechanism of this model remains to be determined. Several lines of evidence point to Fbh1 being involved in preventing the formation of recombination intermediates following replication blockage. The formation of such recombination intermediates (Fig. 7; transition from C to E) could explain the phenotypes associated with the inactivation of Fbh1. None of the experimental data presented here indicate that non-crossover-type HR, which accounts for the majority of HR during somatic cell division in vertebrates (18), is increased in the absence of *FBH1*. Neither gene targeting, HR-dependent repair of I-SceI-induced DSBs, nor Ig gene conversion was decreased in frequency in *FBH1*$^{-/-}$ cells.

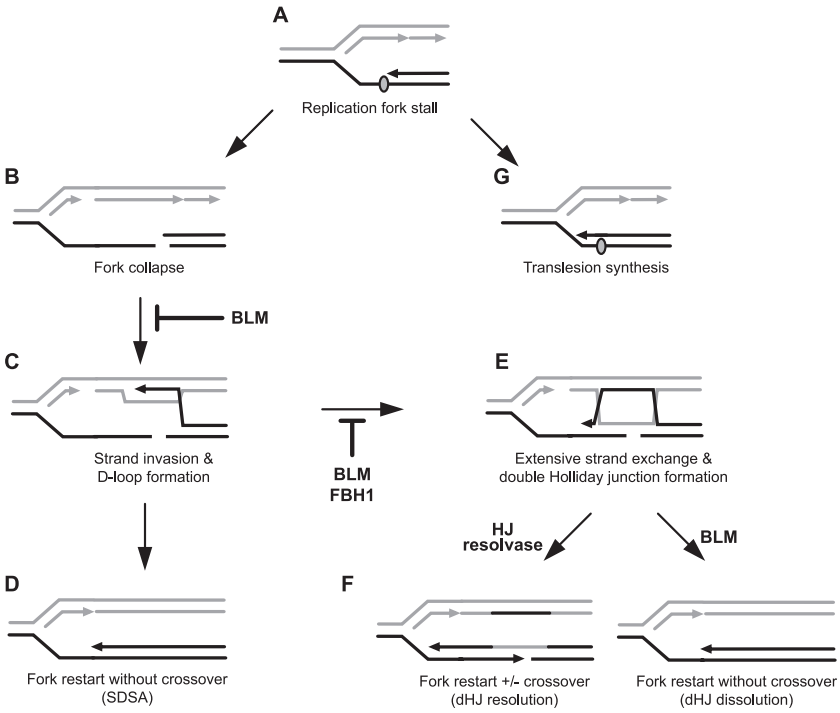

FIG. 7. Model for the function of Fbh1 and Blm at stalled replication forks. A replication fork encounters damages on the template (oval) and is blocked. This block can be bypassed by translesion synthesis (transition from A to G), or the fork can collapse (transition from A to B). HR to restart the collapsed fork is usually carried out by synthesis-dependent strand annealing (SDSA), which is not associated with crossover (transition from C to D). More extensive strand exchange between sister chromatids (E) leads to the formation of a double Holliday junction, which may be resolved with crossover (F). Blm may play a number of roles that reduce crossovers. It may suppress D-loop formation (transition from B to C) (40), reverse Holliday junction formation (transition from C to E) (26) and, with topoisomerase IIIα, promote the dissolution of double Holliday junctions, thereby avoiding resolution by incision (42). The present data support a role for Fbh1 acting alongside Blm in the second of these possibilities, the avoidance of extensive strand exchange and Holliday junction formation (transition from C to E).

Deletion of *FBH1* had no effect on sensitivity to UV, MMS, and cisplatin, which block replication and induce recombination, even in the absence of *BLM*. Thus, it does not seem likely that Fbh1 processes putative recombination intermediates (such as the chicken foot or double Holliday junction) directly. Despite a lack of evidence for a general increase in HR events in *FBH1*$^{-/-}$ cells, *FBH1* deficiency leads to a significant increase in the number of crossovers between homologous chromosomes (radial structures) after UV irradiation. This, coupled with an increased level of camptothecin-induced chromosome-type breaks in *FBH1*$^{-/-}$ *RAD54*$^{-/-}$ cells, indicates that sister-mediated HR-dependent repair is blocked after physical interactions of two sister chromatids in the absence of Fbh1. Such a defect in the suppression of processing recombination intermediates in *FBH1*$^{-/-}$ cells after DNA damage accords with the phenotype of *S. pombe Fbh1* cells (27). In conclusion, Fbh1 is likely to prevent extensive exchange between two homologous sequences, thereby facilitating HR-dependent repair of single-ended breaks formed during replication.

Fbh1 and Blm act in parallel in the repair of DSBs that occur as a consequence of replication block. The present study reveals phenotypic similarities as well as differences in the mutant phenotype of the *FBH1* orthologs of DT40 and *S. pombe*. In both species, deletion of the *FBH1* gene augments the phenotype of *BLM*$^{-/-}$/*rqh1* mutants. On the other hand, *FBH1*$^{-/-}$ cells did not show a prominent phenotype, while *S. pombe fbh1* mutants exhibit sensitivity to variety of DNA damaging agents and enhanced Rad51 focus formation. Thus, the prominent role of Fbh1 in *S. pombe* is not seen in DT40, suggesting that either vertebrate cells have a reduced requirement for this helicase or the functions of Fbh1 can be covered by other helicases as well as Blm. *BLM*-deficient cells are characterized by hyper-recombination between sister chromatids and also between homologous chromosomes (7). These phenotypes were also observed, although to a lesser degree, in *FBH1*$^{-/-}$ cells (Fig. 3C and D and 6E). It should be noted that the *FBH1* mutation increased the sensitivity of *BLM*$^{-/-}$ cells to camptothecin but not to any other damaging agents (Fig. 5 B to D). Spontaneous single-strand nicks are likely to collapse replication forks to produce single-ended breaks similar to those induced by camptothecin (Fig. 7B) (33). These single-ended breaks trigger recombination-mediated replication restart, hence a requirement for Rad54, explaining the additive compromise in genomic stability and sensitivity to camptothecin in the *FBH1*$^{-/-}$ *RAD54*$^{-/-}$ double mutant. Thus, the absence of Fbh1 or Blm may cause an accumulation of recombination intermediates that normally require these DNA helicases for their resolution. The synergistic effect of disruption of *RAD54* in both *FBH1*$^{-/-}$ and *BLM*$^{-/-}$ cells provides further support for a functional similarity between Fbh1 and Blm (41).

Taking our results together, we conclude that the Fbh1-dependent pathway is likely to act in parallel to Blm in cellular

tolerance of single-ended breaks resulting from replication blocks. In humans, Fbh1 may play a role in suppression of the loss of heterozygosity, like Blm, thereby preventing tumor formation. No human *FBH1* mutants have been reported, possibly because *FBH1* disruption alone does not result in a clinically detectable syndrome or, although less likely given the lack of a phenotype in DT40 cells, is lethal. However, it will be interesting to determine whether a defect in this helicase function is associated with cancer predisposition or even a genetic disease akin to Bloom's and Werner's syndromes.

ACKNOWLEDGMENTS

We thank the members of the Takeda laboratories for help and support. Special thanks go to Y. Sato, M. Nakaoka, and R. Ohta for technical assistance. We also thank M. Seki (Tohoku University) for helpful discussions and M. C. Whitby (University of Oxford) for critical reading and discussion.

Financial support was provided in part by a grant from Core Research for Evolutional Science and Technology (CREST) of Japan Science and Technology Corporation; by a Center of Excellence (COE) grant to S.T.; by a Grant-In-Aid for Priority Areas to H.S. for Scientific Research from the Ministry of Education, Culture, Sports, Science and Technology of Japan; and by grants from The Uehara Memorial Foundation and The Naito Foundation.

REFERENCES

1. **Adachi, N., S. So, and H. Koyama.** 2004. Loss of nonhomologous end joining confers camptothecin resistance in DT40 cells. Implications for the repair of topoisomerase I-mediated DNA damage. J. Biol. Chem. **279:**37343–37348.
2. **Alexeev, A., A. Mazin, and S. C. Kowalczykowski.** 2003. Rad54 protein possesses chromatin-remodeling activity stimulated by the Rad51-ssDNA nucleoprotein filament. Nat. Struct. Biol. **10:**182–186.
3. **Arakawa, H., D. Lodygin, and J. M. Buerstedde.** 2001. Mutant loxP vectors for selectable marker recycle and conditional knock-outs. BMC Biotechnol. **1:**7.
4. **Arnaudeau, C., C. Lundin, and T. Helleday.** 2001. DNA double-strand breaks associated with replication forks are predominantly repaired by homologous recombination involving an exchange mechanism in mammalian cells. J. Mol. Biol. **307:**1235–1245.
5. **Bezzubova, O., A. Silbergleit, Y. Yamaguchi-Iwai, S. Takeda, and J. M. Buerstedde.** 1997. Reduced X-ray resistance and homologous recombination frequencies in a RAD54$^{-/-}$ mutant of the chicken DT40 cell line. Cell **89:**185–193.
6. **Buerstedde, J. M., C. A. Reynaud, E. H. Humphries, W. Olson, D. L. Ewert, and J. C. Weill.** 1990. Light chain gene conversion continues at high rate in an ALV-induced cell line. EMBO J. **9:**921–927.
7. **Chakraverty, R. K., and I. D. Hickson.** 1999. Defending genome integrity during DNA replication: a proposed role for RecQ family helicases. Bioessays **21:**286–294.
8. **Doe, C. L., and M. C. Whitby.** 2004. The involvement of Srs2 in post-replication repair and homologous recombination in fission yeast. Nucleic Acids Res. **32:**1480–1491.
9. **Ellis, N. A., and J. German.** 1996. Molecular genetics of Bloom's syndrome. Hum. Mol. Genet. **5:**1457–1463.
10. **Fujimori, A., S. Tachiiri, E. Sonoda, L. H. Thompson, P. K. Dhar, M. Hiraoka, S. Takeda, Y. Zhang, M. Reth, and M. Takata.** 2001. Rad52 partially substitutes for the Rad51 paralog XRCC3 in maintaining chromosomal integrity in vertebrate cells. EMBO J. **20:**5513–5520.
11. **Fukushima, T., M. Takata, C. Morrison, R. Araki, A. Fujimori, M. Abe, K. Tatsumi, M. Jasin, P. K. Dhar, E. Sonoda, T. Chiba, and S. Takeda.** 2001. Genetic analysis of the DNA-dependent protein kinase reveals an inhibitory role of Ku in late S-G$_2$ phase DNA double-strand break repair. J. Biol. Chem. **276:**44413–44418.
12. **Hickson, I. D.** 2003. RecQ helicases: caretakers of the genome. Nat. Rev. Cancer **3:**169–178.
13. **Hirano, S., K. Yamamoto, M. Ishiai, M. Yamazoe, M. Seki, N. Matsushita, M. Ohzeki, Y. M. Yamashita, H. Arakawa, J. M. Buerstedde, T. Enomoto, S. Takeda, L. H. Thompson, and M. Takata.** 2005. Functional relationships of FANCC to homologous recombination, translesion synthesis, and BLM. EMBO J. **24:**418–427.
14. **Hochegger, H., D. Dejsuphong, T. Fukushima, C. Morrison, E. Sonoda, V. Schreiber, G. Y. Zhao, A. Saberi, M. Masutani, N. Adachi, H. Koyama, G. de Murcia, and S. Takeda.** 2006. Parp-1 protects homologous recombination from interference by Ku and ligase IV in vertebrate cells. EMBO J. **25:**1305–1314.
15. **Hochegger, H., E. Sonoda, and S. Takeda.** 2004. Post-replication repair in DT40 cells: translesion polymerases versus recombinases. Bioessays **26:**151–158.
16. **Hoeijmakers, J. H.** 2001. Genome maintenance mechanisms for preventing cancer. Nature **411:**366–374.
17. **Imamura, O., K. Fujita, C. Itoh, S. Takeda, Y. Furuichi, and T. Matsumoto.** 2002. Werner and Bloom helicases are involved in DNA repair in a complementary fashion. Oncogene **21:**954–963.
18. **Johnson, R. D., and M. Jasin.** 2000. Sister chromatid gene conversion is a prominent double-strand break repair pathway in mammalian cells. EMBO J. **19:**3398–3407.
19. **Johnson, R. D., N. Liu, and M. Jasin.** 1999. Mammalian XRCC2 promotes the repair of DNA double-strand breaks by homologous recombination. Nature **401:**397–399.
20. **Kikuchi, K., Y. Taniguchi, A. Hatanaka, E. Sonoda, H. Hochegger, N. Adachi, Y. Matsuzaki, H. Koyama, D. C. van Gent, M. Jasin, and S. Takeda.** 2005. Fen-1 facilitates homologous recombination by removing divergent sequences at DNA break ends. Mol. Cell. Biol. **25:**6948–6955.
21. **Kim, J., J. H. Kim, S. H. Lee, D. H. Kim, H. Y. Kang, S. H. Bae, Z. Q. Pan, and Y. S. Seo.** 2002. The novel human DNA helicase hFBH1 is an F-box protein. J. Biol. Chem. **277:**24530–24537.
22. **Kim, J. H., J. Kim, D. H. Kim, G. H. Ryu, S. H. Bae, and Y. S. Seo.** 2004. SCFhFBH1 can act as helicase and E3 ubiquitin ligase. Nucleic Acids Res. **32:**2287–2297.
23. **Lindahl, T.** 1993. Instability and decay of the primary structure of DNA. Nature **362:**709–715.
24. **Liu, Y., and S. C. West.** 2004. Happy Hollidays: 40th anniversary of the Holliday junction. Nat. Rev. Mol. Cell Biol. **5:**937–944.
25. **Metzger, D., J. Clifford, H. Chiba, and P. Chambon.** 1995. Conditional site-specific recombination in mammalian cells using a ligand-dependent chimeric Cre recombinase. Proc. Natl. Acad. Sci. USA **92:**6991–6995.
26. **Mohaghegh, P., J. K. Karow, R. M. Brosh Jr., V. A. Bohr, and I. D. Hickson.** 2001. The Bloom's and Werner's syndrome proteins are DNA structure-specific helicases. Nucleic Acids Res. **29:**2843–2849.
27. **Morishita, T., F. Furukawa, C. Sakaguchi, T. Toda, A. M. Carr, H. Iwasaki, and H. Shinagawa.** 2005. Role of the *Schizosaccharomyces pombe* F-Box DNA helicase in processing recombination intermediates. Mol. Cell. Biol. **25:**8074–8083.
28. **Okada, T., E. Sonoda, Y. M. Yamashita, S. Koyoshi, S. Tateishi, M. Yamaizumi, M. Takata, O. Ogawa, and S. Takeda.** 2002. Involvement of vertebrate polkappa in Rad18-independent postreplication repair of UV damage. J. Biol. Chem. **277:**48690–48695.
29. **Osman, F., J. Dixon, A. R. Barr, and M. C. Whitby.** 2005. The F-Box DNA helicase Fbh1 prevents Rhp51-dependent recombination without mediator proteins. Mol. Cell. Biol. **25:**8084–8096.
30. **Paques, F., and J. E. Haber.** 1999. Multiple pathways of recombination induced by double-strand breaks in *Saccharomyces cerevisiae*. Microbiol. Mol. Biol. Rev. **63:**349–404.
31. **Petukhova, G., S. Stratton, and P. Sung.** 1998. Catalysis of homologous DNA pairing by yeast Rad51 and Rad54 proteins. Nature **393:**91–94.
32. **Ralf, C., I. D. Hickson, and L. Wu.** 2006. The Bloom's syndrome helicase can promote the regression of a model replication fork. J. Biol. Chem. **281:**22839–22846.
33. **Saleh-Gohari, N., H. E. Bryant, N. Schultz, K. M. Parker, T. N. Cassel, and T. Helleday.** 2005. Spontaneous homologous recombination is induced by collapsed replication forks that are caused by endogenous DNA single-strand breaks. Mol. Cell. Biol. **25:**7158–7169.
34. **Sogo, J. M., M. Lopes, and M. Foiani.** 2002. Fork reversal and ssDNA accumulation at stalled replication forks owing to checkpoint defects. Science **297:**599–602.
35. **Sonoda, E., M. S. Sasaki, J. M. Buerstedde, O. Bezzubova, A. Shinohara, H. Ogawa, M. Takata, Y. Yamaguchi-Iwai, and S. Takeda.** 1998. Rad51-deficient vertebrate cells accumulate chromosomal breaks prior to cell death. EMBO J. **17:**598–608.
36. **Sonoda, E., M. S. Sasaki, C. Morrison, Y. Yamaguchi-Iwai, M. Takata, and S. Takeda.** 1999. Sister chromatid exchanges are mediated by homologous recombination in vertebrate cells. Mol. Cell. Biol. **19:**5166–5169.
37. **Strumberg, D., A. A. Pilon, M. Smith, R. Hickey, L. Malkas, and Y. Pommier.** 2000. Conversion of topoisomerase I cleavage complexes on the leading strand of ribosomal DNA into 5′-phosphorylated DNA double-strand breaks by replication runoff. Mol. Cell. Biol. **20:**3977–3987.
38. **Sugawara, N., X. Wang, and J. E. Haber.** 2003. In vivo roles of Rad52, Rad54, and Rad55 proteins in Rad51-mediated recombination. Mol. Cell **12:**209–219.
39. **Takata, M., M. S. Sasaki, E. Sonoda, C. Morrison, M. Hashimoto, H. Utsumi, Y. Yamaguchi-Iwai, A. Shinohara, and S. Takeda.** 1998. Homologous recombination and non-homologous end-joining pathways of DNA double-strand break repair have overlapping roles in the maintenance of chromosomal integrity in vertebrate cells. EMBO J. **17:**5497–5508.
40. **van Brabant, A. J., T. Ye, M. Sanz, I. J. German, N. A. Ellis, and W. K. Holloman.** 2000. Binding and melting of D-loops by the Bloom syndrome helicase. Biochemistry **39:**14617–14625.

41. **Wang, W., M. Seki, Y. Narita, E. Sonoda, S. Takeda, K. Yamada, T. Masuko, T. Katada, and T. Enomoto.** 2000. Possible association of BLM in decreasing DNA double strand breaks during DNA replication. EMBO J. **19:**3428–3435.
42. **Wu, L., and I. D. Hickson.** 2003. The Bloom's syndrome helicase suppresses crossing over during homologous recombination. Nature **426:**870–874.
43. **Wu, L., and I. D. Hickson.** 2006. DNA helicases required for homologous recombination and repair of damaged replication forks. Annu. Rev. Genet. **40:**279–306.
44. **Yamashita, Y. M., T. Okada, T. Matsusaka, E. Sonoda, G. Y. Zhao, K. Araki, S. Tateishi, M. Yamaizumi, and S. Takeda.** 2002. RAD18 and RAD54 cooperatively contribute to maintenance of genomic stability in vertebrate cells. EMBO J. **21:**5558–5566.